University of Groningen

Brain microstructural development in neonates with critical congenital heart disease

Claessens, Nathalie H. P.; Breur, Johannes M. P. J.; Groenendaal, Floris; Wosten-van Asperen, Roelie M.; Stegeman, Raymond; Haas, Felix; Dudink, Jeroen; de Vries, Linda S.; Jansen, Nicolaas J. G.; Benders, Manon J. N. L.

Link to publication in University of Groningen/UMCG research database

Brain microstructural development in neonates with critical congenital heart disease: An atlas-based diffusion tensor imaging study

Nathalie H.P. Claessens[a,b,c], Johannes M.P.J. Breur[b], Floris Groenendaal[a], Roelie M. Wösten-van Asperen[c], Raymond Stegeman[a,b,c], Felix Haas[d], Jeroen Dudink[a], Linda S. de Vries[a], Nicolaas J.G. Jansen[c,e], Manon J.N.L. Benders[a,*]

[a] *Department of Neonatology, Wilhelmina Children's Hospital, University Medical Center Utrecht, Utrecht, The Netherlands*
[b] *Department of Pediatric Cardiology, Wilhelmina Children's Hospital, University Medical Center Utrecht, Utrecht, The Netherlands*
[c] *Department of Pediatric Intensive Care, Wilhelmina Children's Hospital, University Medical Center Utrecht, Utrecht, The Netherlands*
[d] *Department of Pediatric Cardiothoracic Surgery, Wilhelmina Children's Hospital, University Medical Center Utrecht, Utrecht, The Netherlands*
[e] *Department of Pediatrics, University Medical Center Groningen, Groningen, The Netherlands*

A B S T R A C T

Background: Brain microstructural maturation progresses rapidly in the third trimester of gestation and first weeks of life, but typical microstructural development may be influenced by the presence of critical congenital heart disease (CHD).

Objective: The aim of this study was to investigate the pattern of white matter (WM) microstructural development in neonates with different types of critical CHD. The secondary aim was to examine whether there is an association between WM microstructural maturity and neonatal ischemic brain injury.

Methods: For this prospective, longitudinal cohort study, 74 term born neonates underwent diffusion tensor imaging (DTI) before (N = 56) and after (N = 71) cardiac surgery performed < 30 days of life for transposition of the great arteries (TGA), single ventricle physiology with aortic arch obstruction (SVP-AO), left- (LVOTO) or right ventricle outflow tract obstruction (RVOTO). Microstructural integrity was investigated by fractional anisotropy (FA) and by mean diffusivity (MD) in 16 white matter (WM) structures in three WM regions with correction for postmenstrual age. Ischemic brain injury was defined as moderate-severe white matter injury or stroke.

Results: Before cardiac surgery, the posterior parts of the corona radiata and internal capsule showed significantly higher FA and lower MD compared to the anterior parts. Centrally-located WM structures demonstrated higher FA compared to peripherally-located structures. Neonates with TGA had higher FA in projection-, association- and commissural WM before surgery, when compared to other CHD groups. Neonates with LVOTO showed lower preoperative MD in these regions, and neonates with SVP-AO higher MD. Differences in FA/MD between CHD groups were most clear in centrally located WM structures. Between CHD groups, no differences in postoperative FA/MD or in change from pre- to postoperative FA/MD were seen. Neonatal ischemic brain injury was not associated with pre- or postoperative FA/MD.

Conclusions: Collectively, these findings revealed brain microstructural WM development to follow the same organized pattern in critical CHD as reported in healthy and preterm neonates, from posterior-to-anterior and central-to-peripheral. Neonates with TGA and LVOTO showed the most mature WM microstructure before surgery and SVP-AO the least mature. Degree of WM microstructural immaturity was not associated with ischemic brain injury.

1. Introduction

Neurological problems are common in survivors with critical congenital heart disease (CHD), including cerebral palsy, cognitive delay, behavioral problems and psychiatric disorders.(Latal, 2016; Marelli et al., 2016) In children and adolescents born with critical CHD, brain white matter (WM) microstructural integrity is reduced when compared to healthy controls, and these reductions are associated with poorer

cognitive and executive functioning.(Rollins et al., 2014; Watson et al., 2018; Panigrahy et al., 2015) Several studies have observed that WM microstructural immaturity in critical CHD is already present at neonatal age.(Miller et al., 2007; Ortinau et al., 2012; Makki et al., 2013; Hagmann et al., 2016; Mulkey et al., 2014)

In the last part of gestation, the brain undergoes rapid microstructural changes. In the normal situation, the brain is responsible for 50% of total fetal oxygen consumption.(Prsa et al., 2014) However, in fetuses with critical CHD, cerebral oxygen delivery and oxygen consumption are reduced when compared to healthy fetuses.(Donofrio et al., 2003; Sun et al., 2015) In most cases of critical CHD, the anatomical change causes a mixture of oxygen-rich and oxygen-low blood delivered to the brain, reducing blood oxygen content. In addition, obstruction of the aortic valve or aortic arch can reduce cerebral blood flow.(Claessens et al., 2017)

Diffusion tensor imaging (DTI) allows quantitative analysis of the brain at a microstructural level in vivo.(Feldman et al., 2010) With development, brain water content decreases and WM microstructure becomes more organized with the formation of axonal membranes and myelination. These developmental processes limit the movement of water molecules to certain directions (anisotropic diffusion). Fractional anisotropy (FA) and mean diffusivity (MD) are two DTI based measures used to quantify the integrity of WM microstructure by measuring the degree of anisotropy (FA) and the magnitude of average water diffusion across all directions (MD).(Feldman et al., 2010) With increasing postmenstrual age (PMA), FA increases in the WM and decreases in the cortex, while MD decreases in all brain regions.(Kasprian et al., 2008; Kersbergen et al., 2014)

In typical development, brain microstructural maturation follows a well-established organized pattern, in a posterior-to-anterior and central-to-peripheral direction.(Rose et al., 2014) In critical CHD, it is still unknown if antenatal and postnatal developmental trajectories of brain microstructure follow this same organized pattern and whether there are differences among cardiac defects. Knowledge on the pattern of brain microstructural development in critical CHD will provide a basis for further research investigating the prognostic value of brain microstructural developmental alterations in clinical practice and the development of interventions to improve brain development.

In this study, the aim was to investigate white matter microstructural development in a cohort of term born neonates with critical CHD using atlas-based DTI, related to type of critical CHD. The secondary aim was to evaluate the association between white matter microstructural maturity and neonatal ischemic brain injury.

2. Methods

2.1. Study population

This is a prospective, observational cohort study including neonates with critical CHD who underwent open-heart surgery with the use of cardiopulmonary bypass ≤30 days of life between January 2016 and March 2018 at the Wilhelmina Children's Hospital Utrecht, The Netherlands. As part of standard clinical care, all neonates facing open-heart surgery undergo preoperative (first week of life) and postoperative MRI of the brain (5–10 days after surgery). The following CHD groups were included for this study: transposition of the great arteries (TGA), single ventricle physiology with aortic arch obstruction (SVP-AO), biventricular physiology with left ventricle outflow tract obstruction (LVOTO) and right ventricle outflow tract obstruction (RVOTO). Neonates born < 36 weeks of gestation or with a genetic disorder or major additional congenital anomaly were excluded. The institutional medical ethical review board approved the study and parental informed consent was obtained for the use of clinically obtained data for research purposes.

2.2. Clinical course

Between birth and surgery all neonates were admitted to the pediatric cardiology ward or pediatric intensive care unit (in case of need for respiratory and/or circulatory support). During surgery all patients were positioned in supine position with the head on a gel cushion and a small pillow lifting the chest. Standard anesthetic protocols during surgery included sevoflurane (induction), midazolam and sufentanil (continuous sedation) and pancuronium (muscle paralysis). Postoperative sedation was routinely ensured by midazolam, morphine, and clonidine. By standard protocol all neonates received tranexamic acid 25 mg/kg in 30 min at start of surgery, with afterwards continuation by 10 mg/kg/h during the rest of surgery. At the moment of median sternotomy, heparin 3–4 mg/kg was administered with administration of protamine sulfate 3–4 mg/kg at the end of surgery. Neonates undergoing aortic arch surgery were cooled to a nasopharyngeal temperature of ≈18 °C. Neonates undergoing an arterial switch procedure were cooled to ≈28 °C. Either ante grade cerebral perfusion or deep hypothermic cardiac arrest was chosen as perfusion technique by standard double venous cannulation.

2.3. MRI scanning protocol

All subjects were scanned in a 3.0 T MR system (Philips Medical Systems, Best, Netherlands). Neonates were fed, swaddled in a vacuum cushion and, if necessary, sedated with oral chloral hydrate (50–60 mg/kg). Neonates who required mechanical ventilation at the time of MRI received continuous sedation. Heart rate, oxygen saturation and respiratory rate were monitored. All neonates received three layers of hearing protection (mini muffs, ear muffs and foam cushion around the coil). Scanning protocol included: volumetric 3D T1 weighted imaging (TE/TR = 4.7/9.7 ms, FOV = 200x200x132mm, slice thickness = 1.2 mm without gap), coronal T2 weighted imaging (TE/TR = 150/4851 ms, FOV = 180x180x132mm, slice thickness = 1.2 mm without gap), axial diffusion weighted imaging (b-value = 1000, TE/TR = 66/6493 ms, FOV = 160x182x132mm, slice thickness = 2 mm without gap), axial susceptibility weighted imaging (TE/TR = 30/53 ms, FOV = 160x144x90, slice thickness = 2 mm without gap). All MR images were scored for ischemic brain injury: moderate-severe white matter injury (WMI, > 3 lesions < 2 mm, ≥2 lesions ≥2 mm) and stroke (single white matter lesion ≥2 mm or stroke with cortical or deep grey matter involvement). All MR images were scored independently by two reviewers with experience in neonatal neurology blinded for clinical course.

The DTI protocol consisted of a single-shot spin-echo echoplanar imaging sequence (TR/TE = 6500/80 ms, FOV = 160x160x90mm, acquisition matrix = 80x78mm, reconstruction matrix = 80x80mm, slice thickness = 2 mm without gap), acquired in the axial plane with diffusion gradients applied in 45 directions with a b-value of 800 s/mm2 and one non-diffusion weighted image.

2.4. DTI analysis

DTI data were analyzed using the DTI toolbox ExploreDTI (http://www.exploredti.com/).(Leemans et al., 2009) Data were corrected for subject motion and eddy current induced distortions.(Leemans and Jones, 2009) Tensor estimation was performed using the REKINDLE approach for outliers.(Tax et al., 2015) Automated atlas based analysis with registration to the JHU neonatal brain atlas (http://cmrm.med.jhmi.edu/),(Oishi et al., 2011) using both affine and elastic transformation, was performed for all subjects. All data were visually inspected in terms of quality of tensor estimation, motion correction and template registration using the outlier profile inspection tools embedded within the DTI toolbox ExploreDTI. (Leemans et al., 2009) FA and MD were calculated in the 122 brain structures provided by the JHU neonatal brain atlas, 61 structures per hemisphere, of which 16 white matter
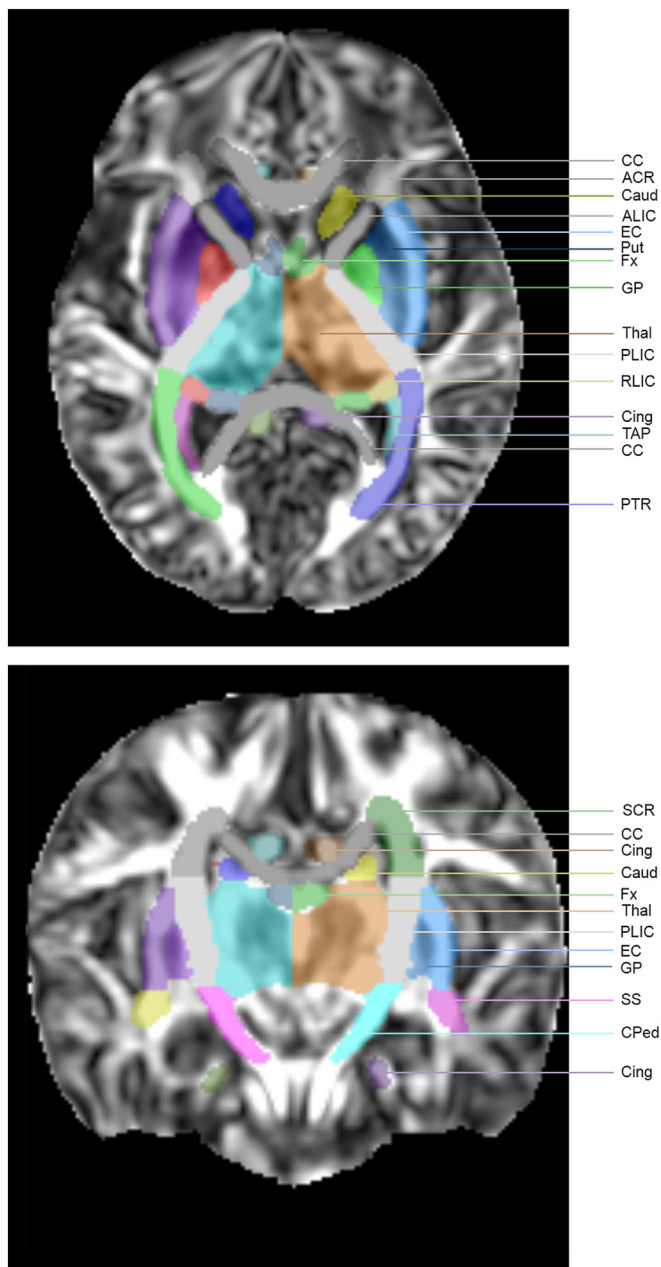
Fig. 1. Diffusion tensor imaging atlas-based template. Template shows the sixteen selected white matter structures: anterior (ACR), superior (SCR), and posterior (PCR) corona radiata, anterior (ALIC) and posterior (PLIC) internal capsule, retrolenticular part of the internal capsule (RLIC), posterior thalamic radiation (PTR), sagittal striatum (SS), external capsule (EC), cerebral peduncle (CPed), superior longitudinal fasciculus (SLF), corpus callosum (CC), tapetum (TAP), inferior (IFOF) and superior fronto-occipital fasciculus (SFOF) and two additional white matter structures that were not included in the analysis, fornix (Fx) and cingulum (Cing), as also four deep grey matter regions: putamen (Put), globus pallidus (GP), caudate nucleus (Caud) and thalamus (Thal).(Oishi et al., 2011).

structures were chosen for this study (Fig. 1).(Oishi et al., 2011) Three overall white matter regions were identified: projection WM, association WM and commissural WM (Supplemental Table 1).

2.5. Statistical analysis

Statistical calculations were performed with IBM SPSS ® version 25.0 (SPSS, Chicago, IL) and R ® v. 3.5.0 (R Foundation for Statistical

Computing, Vienna, Austria). Clinical variables were predominantly not normally distributed, therefore medians (interquartile range) were presented for continuous data. Counts (percentage) were presented for categorical data. Left and right FA and MD values for each structure and region were averaged. To assess anterior versus posterior and central versus peripheral differences, and to assess differences between CHD subgroups, FA and MD values were compared between regions using paired *t*-tests, with Bonferroni correction for multiple comparisons. Multivariable regression analysis was performed to test the association between CHD group (independent variable) and white matter structure FA or MD (dependent variable), controlling for PMA at scan. Multivariable linear regression analyses were performed to test the correlation of FA and MD with clinical factors (selected based on previous literature), including birth weight (z-score), gender, Apgar score, postnatal diagnosis, low cardiac output syndrome, controlling for PMA at scan. Very strong correlations were seen between gestational age at birth and PMA at postnatal (preoperative) MRI (r = 0.886, p = .03*10^{-18}) and therefore gestational age at birth was not taken into account as clinical variable. For all tests, *p*-value was corrected for multiple comparisons using Bonferroni correction.

3. Results

Seventy-nine neonates with critical CHD fulfilled the inclusion criteria, of which 74 were included in this study (five died without MRI): 56 had preoperative DTI available (five had surgery at first day of life, four had DTI with a different scan protocol, nine were too unstable for preoperative MRI), 71 had postoperative MRI (two died, one had poor quality DTI), 53 had both preoperative and postoperative DTI available. Demographics and cardiac parameters of 74 included neonates are presented in Table 1. No differences in PMA at time of birth or MRI were seen between CHD groups. Average preoperative FA and MD values for all brain structures and association with PMA are provided in Supplemental Table 1.

Table 1
Demographics and cardiac parameters.

Total group of patients	N = 74
Female	25 (34)
Gestational age	39.5 (38.7–40.6)
Birth weight	3400 (2980–3800)
Birth weight z-score	−0.25 (−0.77–0.46)
Prenatal CHD diagnosis	55 (74)
CHD subtype	
TGA	26 (35)
SVP-AO	17 (23)
LVOTO	19 (26)
RVOTO	12(16)
Preoperative ischemic brain injury	14 (25)
WMI, moderate-severe	12 (21)
Stroke	5 (9)
Preoperative MRI, age in days	5 (3–7)
Preoperative MRI, postmenstrual age in weeks	40.1 (39.4–41.4)
Group of patients with postoperative MRI	N = 71
Postoperative new ischemic brain injury	
New WMI, moderate-severe	25 (34)
New Stroke	15 (20)
Postoperative MRI, days after surgery	8 (7–10)
Postoperative MRI, postmenstrual age in weeks	42.1 (41.3–43.3)
Days between pre- and postoperative MRI	14 (8–16)

Median (interquartile range) and number (%) are presented. CHD indicates congenital heart disease; LVOTO, left ventricle outflow tract obstruction; SVP-AO, single ventricle physiology with aortic arch obstruction; TGA, transposition of the great arteries; RVOTO, right ventricle outflow tract obstruction.

Table 2
Comparison DTI values of adjacent white matter structures.

	FA	Comparison to adjacent structure	MD	Comparison to adjacent structure
	Mean	P-value	Mean$*10^{-3}$ (mm²/s)	P-value
A. Posterior-anterior				
Corona radiata				
PCR	0.21 ± 0.03	$0.02*10^{-13}$*	1.37 ± 0.15	0.03
SCR	0.18 ± 0.03	$0.05*10^{-26}$*	1.39 ± 0.15	$0.02*10^{-16}$*
ACR	0.13 ± 0.02		1.49 ± 0.17	
Internal capsule				
PLIC	0.36 ± 0.03	$0.06*10^{-47}$*	1.07 ± 0.08	$0.02*10^{-29}$*
ALIC	0.20 ± 0.02		1.18 ± 0.10	
B. Central to peripheral				
Projection fibers				
PLIC	0.36 ± 0.02	$0.03*10^{-32}$*	1.07 ± 0.08	$0.02*10^{-31}$*
RLIC	0.27 ± 0.02	$0.03*10^{-29}$*	1.20 ± 0.10	$0.09*10^{-36}$*
PTR	0.22 ± 0.02	0.60	1.45 ± 0.12	0.003
SS	0.21 ± 0.02		1.48 ± 0.13	
Projection fibers				
PLIC	0.36 ± 0.02	$0.02*10^{-28}$*	1.07 ± 0.08	$0.01*10^{-23}$*
Cped	0.29 ± 0.02		1.34 ± 0.10	
Long association fibers				
EC	0.17 ± 0.02	$0.04*10^{-22}$*	1.23 ± 0.11	$0.03*10^{-27}$*
SLF	0.14 ± 0.01		1.47 ± 0.15	
Commissural fibers				
CC	0.27 ± 0.03	$0.02*10^{-27}$*	1.47 ± 0.11	$0.06*10^{-22}$*
TAP	0.20 ± 0.02		1.79 ± 0.17	
C. Inferior to superior				
Long association fibers				
IFOF	0.21 ± 0.02	$0.03*10^{-20}$*	1.23 ± 0.13	$0.03*10^{-14}$*
SFOF	0.14 ± 0.03		1.36 ± 0.10	

Preoperative fractional anisotropy (FA) and mean diffusivity (MD) of anterior (ACR), superior (SCR) and posterior (PCR) corona radiata, anterior (ALIC) and posterior (PLIC) internal capsule, retrolenticular part of the internal capsule (RLIC), posterior thalamic radiation (PTR), sagittal striatum (SS), cerebral peduncle (CPed), external capsule (EC), superior longitudinal fasciculus (SLF), corpus callosum (CC), tapetum (TAP), inferior (IFOF) and superior fronto-occipital fasciculus (SFOF) are presented as mean ± SD. Part A. shows the comparison of adjacent structures from anterior to posterior. Part B. from central to peripheral and Part C. from inferior to superior.

* indicates a significant difference with a p < .003 with Bonferroni correction for multiple comparisons.

3.1. Temporal-spatial orientation of brain microstructural white matter development before surgery in neonates with critical congenital heart disease

The posterior limb of the internal capsule (PLIC, containing motor tracts) consistently demonstrated highest FA and lowest MD values when compared to other WM structures (Table 2). The posterior parts of the corona radiata and internal capsule had significantly higher FA, and lower MD compared to the anterior parts (Table 2, A). FA progressively decreased and MD values increased among the projection fibers (PLIC to sagittal striatum), corresponding to relative spatial orientation of these tracts from central to peripheral (Table 2, B). Centrally-located association fibers of the external capsule had significantly higher FA and lower MD than the superior longitudinal fasciculus. Also, centrally-located projection fibers of the PLIC and cerebral peduncle and centrally-located commissural fibers of the corpus callosum demonstrated higher FA compared to peripherally-located association fibers and peripherally located corona radiata. Higher FA and lower MD were seen in the inferior tracts of the fronto-occipital fasciculus compared to the superior tracts (Table 2, C). No differences in spatial orientation of WM structures were seen between CHD groups (Fig. 2).

3.2. Differences in preoperative and postoperative white matter microstructure between cardiac defects

In projection, association and commissural WM regions, highest FA values were seen in neonates with TGA when compared to other CHD groups (all p < .001). In multivariable analysis, preoperative FA was associated with CHD group in the internal capsule, cerebral peduncle, inferior and superior fronto-occipital fasciculus, external capsule, uncinate fasciculus, corpus callosum and tapetum (Table 3). Post-hoc analysis showed that neonates with TGA showed significantly higher FA of these WM structures than other CHD groups.

At postoperative time point, no association between CHD group and FA was seen for any WM structure. Neonates with SVP-AO, LVOTO and RVOTO showed significant increase in FA in several WM structures, especially less mature WM structures, where neonates with TGA did not show significant increase in FA over time (Table 3). No association was found between CHD group and percentage of increase in FA from pre- to postoperative time point for any WM structure in multivariable analysis.

MD was lowest in LVOTO and highest in SVP-AO when compared to other CHD groups in projection, association and commissural WM regions (all p < .001). No association was seen between CHD group and preoperative MD, postoperative MD or percentage of increase in MD in multivariable regression analysis. In post-hoc analysis, neonates with LVOTO showed lower preoperative MD values when compared to the other three groups in the following WM structures: anterior and posterior limb of the internal capsule, cerebral peduncle, external capsule and corpus callosum (data not shown).

3.3. Association of brain microstructure with acquired ischemic brain injury

Preoperative moderate-severe WMI was seen in 12 neonates and stroke in five (Table 1). No significant difference in preoperative FA/MD of any WM structure was seen between neonates with and without preoperative WMI (example; FA PLIC mean 0.355 and 0.357, respectively, p = .68). Between neonates with and without preoperative stroke, no differences were seen in FA/MD of WM structures (example; FA PLIC mean 0.362 and 0.356 respectively, p = .85). In addition, no differences in postoperative FA/MD were seen for neonates with new WMI or new stroke (data not shown). Increase in overall WM FA was lower in neonates with ischemic brain injury when compared to neonates without ischemic brain injury (+1.5% versus +2.3%, p = .001). However, no differences in increase in FA/MD were seen when specified per WM structure between neonates with and without ischemic brain injury (data not shown).

3.4. Association preoperative white matter microstructure and clinical factors

Preoperative PMA at time of scan was associated with preoperative FA in all WM structures. Postoperatively, an association between postoperative PMA was only still seen for superiorly and anteriorly located WM structures (Table 3). Multivariable analyses showed no significant correlations of gender, birth weight z-score, Apgar score, postnatal diagnosis or low cardiac output syndrome with average preoperative FA/MD values (data not shown). Within the group with preoperative low cardiac output syndrome (N = 15, 27%), no differences in FA/MD of any WM structure were seen between the neonates developing WMI and neonates without WMI (data not shown).

4. Discussion

This study examined white matter microstructural development before and after cardiac surgery in a longitudinal cohort of neonates with critical CHD, using atlas-based DTI analysis which has previously been described as a sensitive method to examine neonatal brain
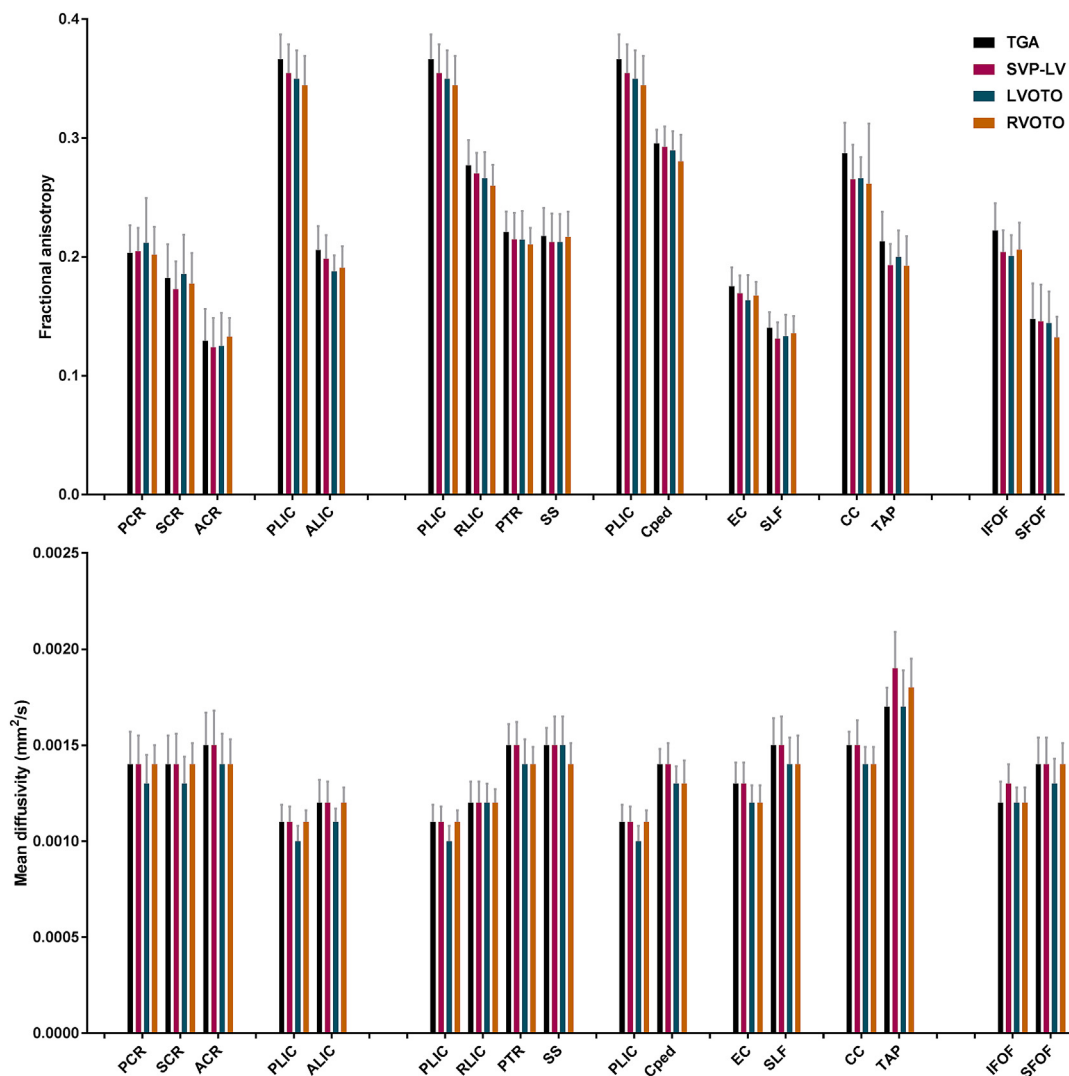
Fig. 2. Preoperative white matter microstructure. Mean fractional anisotropy (top, box) and mean diffusivity (bottom, box) with standard deviation (whiskers) in all white matter (WM) structures for neonates with transposition of the great arteries (TGA), single ventricle physiology with aortic arch obstruction (SVP-AO), left (LVOTO) and right ventricle outflow tract obstruction (RVOTO). Examined WM structures: Anterior (ACR), superior (SCR), and posterior (PCR) corona radiata, anterior (ALIC) and posterior (PLIC) internal capsule, retrolenticular part of the internal capsule (RLIC), posterior thalamic radiation (PTR), sagittal striatum (SS), cerebral peduncle (CPed), external capsule (EC), superior longitudinal fasciculus (SLF), inferior (IFOF) and superior fronto-occipital fasciculus (SFOF), corpus callosum (CC), tapetum (TAP).

microstructure.(Kersbergen et al., 2014; Oishi et al., 2011) In contrast to most DTI studies in neonates with critical CHD, our study uses a whole brain automated atlas-based approach, rather than manually selecting specific white matter regions, gaining a more detailed impression into differential microstructural brain development between different cardiac defects. This is an important first step to identifying microstructural changes that could provide early prognostic biomarkers or guide neuroprotective interventions.

Previous studies have shown neonatal brain immaturity in all critical CHD groups when compared to healthy neonates. (Miller et al., 2007; Ortinau et al., 2012; Makki et al., 2013; Hagmann et al., 2016; Mulkey et al., 2014) This study describes three primary observations on brain microstructural maturity in neonates with critical CHD. Firstly, we observed more mature WM microstructure (i.e. higher FA and lower MD) in posterior compared to anterior, in central compared to peripheral, and in inferior compared to superior WM structures. These findings revealed brain microstructural development to follow the same organized pattern in critical CHD as reported in preterm and healthy neonates.(Kersbergen et al., 2014; Rose et al., 2014; Oishi et al., 2011; Deoni et al., 2011) Secondly, different levels of maturity in

microstructural integrity were seen between CHD groups, with TGA and LVOTO showing the most mature WM microstructure and SVP the least mature. These findings might reflect the different degree of disturbance in antenatal brain development by changes in cerebral blood flow and oxygen delivery among cardiac defects. The order of most mature to least mature white matter structures was not different between cardiac defects. Thirdly, degree of brain microstructural immaturity was not related to ischemic brain injury, either before or after open-heart surgery. Although previous studies have suggested that brain immaturity increases the risk to acquire brain injury in neonates with critical CHD, (Mulkey et al., 2014; Dimitropoulos et al., 2013) our results based on FA/MD do not suggest such a relationship.

Preoperative DTI measurements obtained during the first days of life in neonates with critical CHD reflect antenatal brain microstructural development. A high degree of agreement in the relative order of regions from low-high FA and high-low MD was seen between our population of critical CHD and previous reports in extremely preterm infants and healthy neonates.(Kersbergen et al., 2014; Rose et al., 2014; Oishi et al., 2011; Deoni et al., 2011; Cowan and de Vries, 2005) This suggests that reduced fetal brain oxygen delivery and oxygen

Table 3

Preoperative and postoperative white matter fractional anisotropy stratified by congenital heart defect.

Fractional anisotropy	Association Pre	Association Post	TGA Pre Mean ± SD	TGA Post Mean ± SD	SVP-AO Pre Mean ± SD	SVP-AO Post Mean ± SD	LVOTO Pre Mean ± SD	LVOTO Post Mean ± SD	RVOTO Pre Mean ± SD	RVOTO Post Mean ± SD
Projection fibers										
PLIC	PMA, CHD group		0.372 ± 0.03	0.374 ± 0.03	0.353 ± 0.03	0.378 ± 0.03	0.361 ± 0.03	0.364 ± 0.04	0.350 ± 0.02	0.384 ± 0.03*
Cped	PMA, CHD group		0.301 ± 0.02	0.304 ± 0.02	0.291 ± 0.02	0.302 ± 0.02	0.299 ± 0.02	0.299 ± 0.02	0.285 ± 0.02	0.306 ± 0.02*
RLIC	PMA, CHD group		0.278 ± 0.03	0.279 ± 0.03	0.269 ± 0.02	0.283 ± 0.03	0.274 ± 0.03	0.274 ± 0.04	0.264 ± 0.02	0.287 ± 0.03*
PTR	PMA	PMA	0.225 ± 0.02	0.222 ± 0.03	0.214 ± 0.03	0.221 ± 0.03	0.221 ± 0.03	0.217 ± 0.03	0.214 ± 0.02	0.226 ± 0.02
SS	PMA	PMA	0.220 ± 0.03	0.223 ± 0.03	0.212 ± 0.03	0.221 ± 0.03	0.219 ± 0.03	0.220 ± 0.04	0.221 ± 0.03	0.239 ± 0.03*
PCR	PMA	PMA	0.208 ± 0.03	0.210 ± 0.03	0.204 ± 0.02	0.214 ± 0.02	0.219 ± 0.04	0.233 ± 0.03*	0.205 ± 0.03	0.222 ± 0.03*
ALIC	PMA, CHD group	PMA	0.211 ± 0.03	0.211 ± 0.03	0.198 ± 0.03	0.219 ± 0.03*	0.194 ± 0.02	0.203 ± 0.02*	0.194 ± 0.02	0.221 ± 0.02*
SCR	PMA	PMA	0.186 ± 0.03	0.188 ± 0.03	0.172 ± 0.03	0.184 ± 0.03*	0.192 ± 0.03	0.207 ± 0.05*	0.181 ± 0.03	0.199 ± 0.03*
ACR	PMA	PMA	0.134 ± 0.03	0.136 ± 0.03	0.124 ± 0.03	0.141 ± 0.03*	0.129 ± 0.03	0.143 ± 0.03*	0.135 ± 0.02	0.157 ± 0.03*
Long association fibers										
IFOF	PMA, CHD group		0.222 ± 0.03	0.220 ± 0.02	0.203 ± 0.02	0.208 ± 0.03	0.207 ± 0.02	0.196 ± 0.04	0.209 ± 0.02	0.220 ± 0.02
UF	PMA, CHD group		0.209 ± 0.03	0.204 ± 0.03	0.191 ± 0.03	0.193 ± 0.03	0.189 ± 0.03	0.174 ± 0.05	0.186 ± 0.02	0.198 ± 0.02
EC	PMA, CHD group	PMA	0.177 ± 0.03	0.177 ± 0.03	0.169 ± 0.02	0.177 ± 0.03	0.169 ± 0.02	0.180 ± 0.02	0.170 ± 0.02	0.181 ± 0.02
SFOF	PMA, CHD group	PMA	0.152 ± 0.03	0.159 ± 0.03	0.146 ± 0.03	0.166 ± 0.04*	0.149 ± 0.03	0.177 ± 0.05*	0.134 ± 0.02	0.167 ± 0.03*
SLF	PMA	PMA	0.144 ± 0.02	0.141 ± 0.02	0.131 ± 0.02	0.132 ± 0.02	0.138 ± 0.02	0.148 ± 0.04	0.138 ± 0.02	0.144 ± 0.03
Commissural fibers										
CC	PMA, CHD group		0.290 ± 0.03	0.278 ± 0.03	0.264 ± 0.03	0.265 ± 0.03	0.274 ± 0.02	0.257 ± 0.03	0.264 ± 0.04	0.271 ± 0.03
TAP	PMA, CHD group		0.218 ± 0.03	0.218 ± 0.03	0.192 ± 0.03	0.204 ± 0.03	0.206 ± 0.02	0.197 ± 0.03	0.195 ± 0.02	0.210 ± 0.03*

Order of WM structures per WM region from high-low FA as based on the total CHD population. Multivariable linear regression analysis, with postmenstrual age (PMA) at time of scan included, was performed to examine the association between CHD group and FA; significant associations are indicated in the second and third column. Preoperative and postoperative fractional anisotropy (FA, presented as mean ± SD) of anterior (ACR), superior (SCR),and posterior (PCR) corona radiata, anterior (ALIC) and posterior (PLIC) internal capsule, retrolenticular part of the internal capsule (RLIC), posterior thalamic radiation (PTR), sagittal striatum (SS), cerebral peduncle (CPed), external capsule (EC), superior longitudinal fasciculus (SLF), corpus callosum (CC), tapetum (TAP), inferior (IFOF) and superior fronto-occipital fasciculus (SFOF). Pre indicates preoperative, Post indicates postoperative. CHD indicates congenital heart disease; LVOTO, left ventricle outflow tract obstruction; SVP-AO, single ventricle physiology with aortic arch obstruction; TGA, transposition of the great arteries; RVOTO, right ventricle outflow tract obstruction.

* Indicates significant change from preoperative to postoperative time point within this CHD group; percentage of change was not associated with CHD group or PMA for any WM structure. A p < .0031 with Bonferroni correction for multiple comparisons per CHD group was considered significant.

consumption in critical CHD affects global brain microstructural maturation rather than the maturation of specific white matter structures. The posterior-to-anterior fashion of brain development has also been shown in brain perfusion studies.(De Vis et al., 2013) Further research might reveal whether there is an association between brain perfusion development and brain microstructural development in fetuses and neonates with critical CHD.

Over the last years several studies found lower WM FA before surgery in neonates with critical CHD in the overall WM,(Miller et al., 2007; Ortinau et al., 2012; Mulkey et al., 2014) and specifically in the corpus callosum,(Makki et al., 2013; Hagmann et al., 2016) when compared to healthy neonates. In fetal life, pre-myelinating oligodendrocytes (immature oligodendrocytes) are the most dominant type of oligodendrocytes in the human white matter.(Back et al., 2001) Pre-myelinating oligodendrocytes are vulnerable to hypoxia and after hypoxic-ischemic injury pre-myelinating oligodendrocytes fail to mature to myelin-producing oligodendrocytes, resulting in impaired myelination of the white matter axons.(Volpe, 2014; Volpe, 2011; Volpe et al., 2011; Back et al., 2005) This explains the particular vulnerability of the white matter for microstructural immaturity in fetuses with critical CHD who are suffering reduced cerebral blood flow and blood oxygen content when compared to healthy fetuses.(Sun et al., 2015) Differences in microstructural maturity between CHD groups were more clear in centrally than in peripherally located WM structures, supporting the hypothesis that brain immaturity finds its onset at the earliest stages of brain microstructural development.

In this study, neonates with TGA showed higher FA values in the majority of WM structures when compared to neonates with SVP-AO, LVOTO or RVOTO. This might indicate that the reduction in antenatal cerebral blood flow affects brain microstructural integrity as measured by FA to a higher degree than decreased cerebral blood oxygen content alone, as neonates with TGA have a severe reduction in cerebral blood oxygen content but do have less disturbance in cerebral blood flow than SVP-AO and LVOTO.(Donofrio et al., 2003; Sun et al., 2015) This is supported by a previous study showing more severe brain microstructural immaturity to be associated with smaller aortic diameter. (Sethi et al., 2013) In neonates with TGA, aortic size is not impacted, where aortic arch obstruction is the main problem in SVP-AO and LVOTO. Interestingly, neonates with LVOTO showed the most mature WM microstructure as measured by MD. The majority of fetuses with LVOTO has close to normal in utero blood oxygen saturation, especially when compared to TGA and SVP-AO, which might play a role in the extent to which microstructural integrity as measured by MD is impacted.

Several previous studies have suggested that WM immaturity increases the risk of postnatal WMI in neonates with critical CHD.(Mulkey et al., 2014; Dimitropoulos et al., 2013; Andropoulos et al., 2010) One study in critical CHD found lower WM FA values in a small population of neonates with preoperative brain injury (WMI or stroke) when compared to neonates without brain injury.(Mulkey et al., 2014) WMI is suggested to follow the pattern of WM microstructural maturation, with the predominant location of white matter lesions shifting from posterior to anterior with increasing gestation.(Guo et al., n.d.) In neonates with critical CHD, WMI is the most common type of acquired brain injury and most likely caused by acute fluctuations in cerebral perfusion and oxygenation.(Claessens et al., 2017) WMI is associated with poorer outcomes at school-age.(Claessens et al., 2018) In our study, no differences in preoperative FA or MD values of any WM structure were seen between neonates with and without preoperative WMI. Even the PLIC, the most mature WM structure and not involved in WMI in any of the included neonates, did not expose a difference in maturity between neonates with and without WMI. The role of brain immaturity in the onset of ischemic brain injury in neonates with critical CHD remains uncertain and this role might be more dependent on the exposure to postnatal complications such as low cardiac output syndrome.

Changes in DTI are described as linear processes between 37 and 44 weeks PMA.(Oishi et al., 2011; Miller et al., 2002) The percentage of change in FA and MD from preoperative to postoperative time point (14 days time) in our population of neonates with critical CHD is lower than previously reported in extremely preterm infants until 44 weeks. (Kersbergen et al., 2014; Miller et al., 2002) This suggests that the critical intensive care period with major cardiac surgery might further delay brain microstructural development in neonates with critical CHD. Overall, white matter microstructural integrity as measured by FA showed higher increase in neonates without ischemic brain injury than in neonates with ischemic brain injury, although this difference could not be identified in specific white matter structures. The extent to which this brain microstructural developmental delay remains after the neonatal intensive care period into infancy warrants further attention.

Quantifying brain microstructural development in neonates with critical CHD contributes to the understanding of brain developmental trajectories in this population with a high risk of brain immaturity. Future research including longitudinal MRI in healthy individuals is necessary to investigate whether brain microstructural immaturity in neonates with critical CHD extends into childhood. In this perspective, more detailed analysis of white matter networks in relation to ischemic brain injury and neurodevelopmental outcomes seems highly relevant. There are several limitations to this study. Absolute measurements of brain microstructure must be interpreted with caution, as these may be influenced by diffusion model, MRI parameters and brain architecture (crossing fibers may contribute to variation in FA/MD values).(Oishi et al., 2011; Karmacharya et al., 2018) The used neonatal brain atlas was constructed with data from a healthy term population with a different type of MRI scanner and MRI protocol. However, we checked the quality of template registrations and diffusivity measurements for all neonates included in this study and concluded this was sufficient in all cases.

This study examined brain microstructural development in a longitudinal cohort of neonates with critical CHD, using atlas-based DTI analysis. A high degree of agreement in order of WM structures by microstructural maturity was seen between CHD groups and with previous reports in preterm and healthy neonates. Different levels of antenatal disturbance in cerebral blood flow and blood oxygen content might be underlying to the differences in WM microstructural integrity among CHD groups, with TGA and LVOTO showing the most mature WM microstructure and SVP-AO the least mature. This study could not reveal an association between brain WM microstructural maturity and the risk of acquired ischemic brain injury.

Appendix A. Supplementary data

Supplementary data to this article can be found online at https://doi.org/10.1016/j.nicl.2019.101672.

References

Andropoulos, D.B., Hunter, J.V., Nelson, D.P., Stayer, S.A., Stark, A.R., McKenzie, E.D., Heinle, J.S., Graves, D.E., Fraser Jr., C.D., 2010. Brain immaturity is associated with brain injury before and after neonatal cardiac surgery with high-flow bypass and cerebral oxygenation monitoring. J. Thorac. Cardiovasc. Surg. 139, 543–556.

Back, S.A., Luo, N.L., Borenstein, N.S., Levine, J.M., Volpe, J.J., Kinney, H.C., 2001. Late oligodendrocyte progenitors coincide with the developmental window of vulnerability for human perinatal white matter injury. J. Neurosci. 21, 1302–1312.

Back, S.A., Luo, N.L., Mallinson, R.A., O'Malley, J.P., Wallen, L.D., Frei, B., Morrow, J.D., Petito, C.K., Roberts Jr., C.T., Murdoch, G.H., Montine, T.J., 2005. Selective vulnerability of preterm white matter to oxidative damage defined by F2-isoprostanes. Ann. Neurol. 58, 108–120.

Claessens, N.H.P., Kelly, C.J., Counsell, S.J., Benders, M., 2017. Neuroimaging, cardiovascular physiology, and functional outcomes in infants with congenital heart disease. Dev. Med. Child Neurol. 59 (9), 894–902.

Claessens, N.H.P., Algra, S.O., Ouwehand, T.L., Jansen, N.J.G., Schappin, R., Haas, F., Eijsermans, M.J.C., de Vries, L.S., Benders, M., CHD Lifespan Study Group Utrecht, 2018. Perioperative neonatal brain injury is associated with worse school-age neurodevelopment in children with critical congenital heart disease. Dev. Med. Child Neurol. 60 (10), 1052–1058.

Cowan, F.M., de Vries, L.S., 2005. The internal capsule in neonatal imaging. Semin. Fetal Neonatal Med. 10, 461–474.

De Vis, J.B., Petersen, E.T., de Vries, L.S., Groenendaal, F., Kersbergen, K.J., Alderliesten, T., Hendrikse, J., Benders, M.J., 2013. Regional changes in brain perfusion during brain maturation measured non-invasively with arterial spin labeling MRI in neonates. Eur. J. Radiol. 82, 538–543.

Deoni, S.C., Mercure, E., Blasi, A., Gasston, D., Thomson, A., Johnson, M., Williams, S.C., Murphy, D.G., 2011. Mapping infant brain myelination with magnetic resonance imaging. J. Neurosci. 31, 784–791.

Dimitropoulos, A., McQuillen, P.S., Sethi, V., Moosa, A., Chau, V., Xu, D., Brant, R., Azakie, A., Campbell, A., Barkovich, A.J., Poskitt, K.J., Miller, S.P., 2013. Brain injury and development in newborns with critical congenital heart disease. Neurology 81, 241–248.

Donofrio, M.T., Bremer, Y.A., Schieken, R.M., Gennings, C., Morton, L.D., Eidem, B.W., Cetta, F., Falkensammer, C.B., Huhta, J.C., Kleinman, C.S., 2003. Autoregulation of cerebral blood flow in fetuses with congenital heart disease: the brain sparing effect. Pediatr. Cardiol. 24, 436–443.

Feldman, H.M., Yeatman, J.D., Lee, E.S., Barde, L.H., Gaman-Bean, S., 2010. Diffusion tensor imaging: a review for pediatric researchers and clinicians. J. Dev. Behav. Pediatr. 31, 346–356.

Guo, T., Chau, V., Peyvandi, S., Latal, B., McQuillen, P.S., Knirsch, W., Synnes, A., Feldmann, M., Naef, N., Chakravarty, M.M., De Petrillo, A., Duerden, E.G., Barkovich, A.J., Miller, S.P., 2018. White matter injury in term neonates with congenital heart diseases: topology & comparison with preterm newborns. NeuroImage 185, 742–749.

Hagmann, C., Singer, J., Latal, B., Knirsch, W., Makki, M., 2016. Regional microstructural and volumetric magnetic resonance imaging (MRI) abnormalities in the corpus callosum of neonates with congenital heart defect undergoing cardiac surgery. J. Child Neurol. 31, 300–308.

Karmacharya, S., Gagoski, B., Ning, L., Vyas, R., Cheng, H.H., Soul, J., Newberger, J.W., Shenton, M.E., Rathi, Y., Grant, P.E., 2018. Advanced diffusion imaging for assessing normal white matter development in neonates and characterizing aberrant development in congenital heart disease. Neuroimage Clin. 19, 360–373.

Kasprian, G., Brugger, P.C., Weber, M., Krssak, M., Krampl, E., Herold, C., Prayer, D., 2008. In utero tractography of fetal white matter development. NeuroImage 43, 213–224.

Kersbergen, K.J., Leemans, A., Groenendaal, F., van der Aa, N.E., Viergever, M.A., de Vries, L.S., Benders, M.J., 2014. Microstructural brain development between 30 and 40 weeks corrected age in a longitudinal cohort of extremely preterm infants. NeuroImage 103, 214–224.

Latal, B., 2016. Neurodevelopmental outcomes of the child with congenital heart disease. Clin. Perinatol. 43, 173–185.

Leemans, A., Jones, D.K., 2009. The B-matrix must be rotated when correcting for subject motion in DTI data. Magn. Reson. Med. 61, 1336–1349.

Leemans, A., Jeurissen, B., Sijbers, J., Jones, D.K., 2009. ExploreDTI: a graphical toolbox for processing, analyzing, and visualizing diffusion MR data. In: 17th Annual Meeting of Intl Soc Mag Reson Med, pp. 3537.

Makki, M., Scheer, I., Hagmann, C., Liamlahi, R., Knirsch, W., Dave, H., Bernet, V., Batinic, K., Latal, B., 2013. Abnormal interhemispheric connectivity in neonates with D-transposition of the great arteries undergoing cardiopulmonary bypass surgery. AJNR Am. J. Neuroradiol. 34, 634–640.

Marelli, A., Miller, S.P., Marino, B.S., Jefferson, A.L., Newburger, J.W., 2016. Brain in congenital heart disease across the lifespan: the cumulative burden of injury. Circulation 133, 1951–1962.

Miller, S.P., Vigneron, D.B., Henry, R.G., Bohland, M.A., Ceppi-Cozzio, C., Hoffman, C., Newton, N., Partridge, J.C., Ferriero, D.M., Barkovich, A.J., 2002. Serial quantitative diffusion tensor MRI of the premature brain: development in newborns with and without injury. J. Magn. Reson. Imaging 16, 621–632.

Miller, S.P., McQuillen, P.S., Hamrick, S., Xu, D., Glidden, D.V., Charlton, N., Karl, T., Azakie, A., Ferriero, D.M., Barkovich, A.J., Vigneron, D.B., 2007. Abnormal brain development in newborns with congenital heart disease. N. Engl. J. Med. 357, 1928–1938.

Mulkey, S.B., Ou, X., Ramakrishnaiah, R.H., Glasier, C.M., Swearingen, C.J., Melguizo, M.S., Yap, V.L., Schmitz, M.L., Bhutta, A.T., 2014. White matter injury in newborns with congenital heart disease: a diffusion tensor imaging study. Pediatr. Neurol. 51, 377–383.

Oishi, K., Mori, S., Donohue, P.K., Ernst, T., Anderson, L., Buchthal, S., Faria, A., Jiang, H., Li, X., Miller, M.I., van Zijl, P.C., Chang, L., 2011. Multi-contrast human neonatal brain atlas: application to normal neonate development analysis. NeuroImage 56, 8–20.

Ortinau, C., Beca, J., Lambeth, J., Ferdman, B., Alexopoulos, D., Shimony, J.S., Wallendorf, M., Neil, J., Inder, T., 2012. Regional alterations in cerebral growth exist preoperatively in infants with congenital heart disease. J. Thorac. Cardiovasc. Surg. 143, 1264–1270.

Panigrahy, A., Schmithorst, V.J., Wisnowski, J.L., Watson, C.G., Bellinger, D.C., Newburger, J.W., Rivkin, M.J., 2015. Relationship of white matter network topology and cognitive outcome in adolescents with d-transposition of the great arteries. Neuroimage Clin. 7, 438–448.

Prsa, M., Sun, L., van Amerom, J., Yoo, S.J., Grosse-Wortmann, L., Jaeggi, E., Macgowan, C., Seed, M., 2014. Reference ranges of blood flow in the major vessels of the normal human fetal circulation at term by phase-contrast magnetic resonance imaging. Circ. Cardiovasc. Imaging 7, 663–670.

Rollins, C.K., Watson, C.G., Asaro, L.A., Wypij, D., Vajapeyam, S., Bellinger, D.C., DeMaso, D.R., Robertson Jr., R.L., Newburger, J.W., Rivkin, M.J., 2014. White matter microstructure and cognition in adolescents with congenital heart disease. J. Pediatr. 165, 936–44 e1-2.

Rose, J., Vassar, R., Cahill-Rowley, K., Guzman, X.S., Stevenson, D.K., Barnea-Goraly, N., 2014. Brain microstructural development at near-term age in very-low-birth-weight preterm infants: an atlas-based diffusion imaging study. NeuroImage 86, 244–256.

Sethi, V., Tabbutt, S., Dimitropoulos, A., Harris, K.C., Chau, V., Poskitt, K., Campbell, A., Azakie, A., Xu, D., Barkovich, A.J., Miller, S.P., McQuillen, P.S., 2013. Single-ventricle anatomy predicts delayed microstructural brain development. Pediatr. Res. 73, 661–667.

Sun, L., Macgowan, C.K., Sled, J.G., Yoo, S.J., Manlhiot, C., Porayette, P., Grosse-Wortmann, L., Jaeggi, E., McCrindle, B.W., Kingdom, J., Hickey, E., Miller, S., Seed, M., 2015. Reduced fetal cerebral oxygen consumption is associated with smaller brain size in fetuses with congenital heart disease. Circulation 131, 1313–1323.

Tax, C.M., Otte, W.M., Viergever, M.A., Dijkhuizen, R.M., Leemans, A., 2015. REKINDLE: robust extraction of kurtosis INDices with linear estimation. Magn. Reson. Med. 73, 794–808.

Volpe, J.J., 2011. Systemic inflammation, oligodendroglial maturation, and the encephalopathy of prematurity. Ann. Neurol. 70, 525–529.

Volpe, J.J., 2014. Encephalopathy of congenital heart disease- destructive and developmental effects intertwined. J. Pediatr. 164, 962–965.

Volpe, J.J., Kinney, H.C., Jensen, F.E., Rosenberg, P.A., 2011. The developing oligodendrocyte: key cellular target in brain injury in the premature infant. Int. J. Dev. Neurosci. 29, 423–440.

Watson, C.G., Stopp, C., Wypij, D., Bellinger, D.C., Newburger, J.W., Rivkin, M.J., 2018. Altered white matter microstructure correlates with IQ and processing speed in children and adolescents post-fontan. J. Pediatr. 200 140-149.e4.